Numerical Models. Inverse Models. Mesoscale Eddies. Ocean Circulation. Open Ocean Convection. Patch Dynamics. Regional and Shelf Sea Models. Tides. Upper Ocean Time and Space Variability.

Further Reading

Anderson D and Willebrand J (eds) (1989) *Oceanic Circulation Models: Combining Data and Dynamics*. Dordrecht: Kluwer Academic.

Bennett AF (1992) *Inverse Methods in Physical Oceanography. Cambridge Monographs on Mechanics and Applied Mathematics*. Cambridge: Cambridge University Press.

Brasseur P and Nihoul JCJ (eds) (1994) Data assimilation: tools for modelling the ocean in a global change perspective. In: NATO ASI Series, *Series I: Global Environmental Change*, vol. 19. Springer-Verlag, Berlin.

Egbert GD, Bennett AF and Foreman MGG (1994) TOPEX/POSEIDON tides estimated using a global inverse model. *Journal of Geophysical Research* 24: 821–824, 852.

Haidvogel DB and Robinson AR (eds) (1989) Special issue on data assimilation. *Dynamics of Atmospheres and Oceans* 13: 171–517.

Lermusiaux PFJ (1999) Estimation and study of mesoscale variability in the Strait of Sicily. *Dynamics of Atmospheres and Oceans* 29: 255–303.

Lermusiaux PFJ (2001). Evolving the subspace of the three-dimensional multiscale ocean variability: Massachusetts Bay. *Journal of Marine Systems*. In press.

Lermusiaux PFJ and Robinson AR (1999) Data assimilation via error subspace statistical estimation, Part I: Theory and schemes. *Monthly Weather Review* 7: 1385–1407.

Lermusiaux PFJ and AR Robinson (2001). Features of dominant mesoscale variability, circulation patterns and dynamics in the Strait of Sicily. *Deep Sea Research*, Part I. In press.

Malanotte-Rizzoli P and Young RE (1995) Assimilation of global versus local data sets into a regional model of the Gulf Stream system: I. Data effectiveness. *Journal of Geophysical Research* 24: 773–724.

Malanotte-Rizzoli P (ed) (1996) *Modern Approaches to Data Assimilation in Ocean Modeling, Elsevier Oceanography Series*. The Netherlands: Elsevier Science.

Martel F and Wunsch C (1993) The North Atlantic circulation in the early 1980 s – an estimate from inversion of a finite-difference model. *Journal of Physical Oceanography* 23: 898–924.

Miller RN, Zaron EO and Bennett AF (1994) Data assimilation in models with convective adjustment. *Monthly Weather Review* 122: 2607–2613.

Robinson AR, Lermusiaux PFJ and Sloan NQ III (1998) Data assimilation. In: Brink KH and Robinson AR (eds) *The Sea: The Global Coastal Ocean I, Processes and Methods*, vol. 10. New York: John Wiley and Sons.

Robinson AR (1999) Forecasting and simulating coastal ocean processes and variabilities with the Harvard Ocean Prediction System. In: Mooers CNK (ed) *Coastal Ocean Prediction, AGU Coastal and Estuarine Study Series*, pp. 77–100. Washington: AGU Press.

Robinson AR and the LOOPS group (1999). Real-time forecasting of the multidisciplinary coastal ocean with the Littoral Ocean Observing and Predicting System (LOOPS). *Third Conference on Coastal Atmospheric and Oceanic Prediction and Processes* (3-5 Nov. 1999), New Orleans, LA. American Meteorological Society, 30*35.

Robinson AR and Sellschopp J (2000) Rapid assessment of the coastal ocean environment. In: Pinardi N and Woods JD (eds) *Ocean Forecasting: Conceptual Basis and Applications*. London: Springer-Verlag.

Wunsch C (1996) *The Ocean Circulation Inverse Problem*. Cambridge: Cambridge University Press.

DEEP CONVECTION

J. R. N. Lazier, Bedford Institute of Oceanography, Nova Scotia, Canada

doi:10.1006/rwos.2001.0113

Introduction

Density of ocean water generally increases with depth except at the surface where stirring by waves and convection creates a well-mixed homogeneous layer. Breaking waves alone can mix the upper 5–10 m, but convection, forced by an increase in density at the surface via heat loss or evaporation, can greatly increase the mixed layer depth. During winter, heat loss from the surface of the ocean is high and convectively mixed surface layers are the norm in the extratropical oceans. The deepest (> 1500 m) are found in the Labrador Sea, the Greenland Sea, and the Golfe du Lion in the Mediterranean Sea, because of two special features. First, they are near land where cold continental air flows over the water to create the necessary high heat loss. Second, the circulation in each is weakly cyclonic which helps to maintain the convecting water where the high heat loss occurs. The combination of these

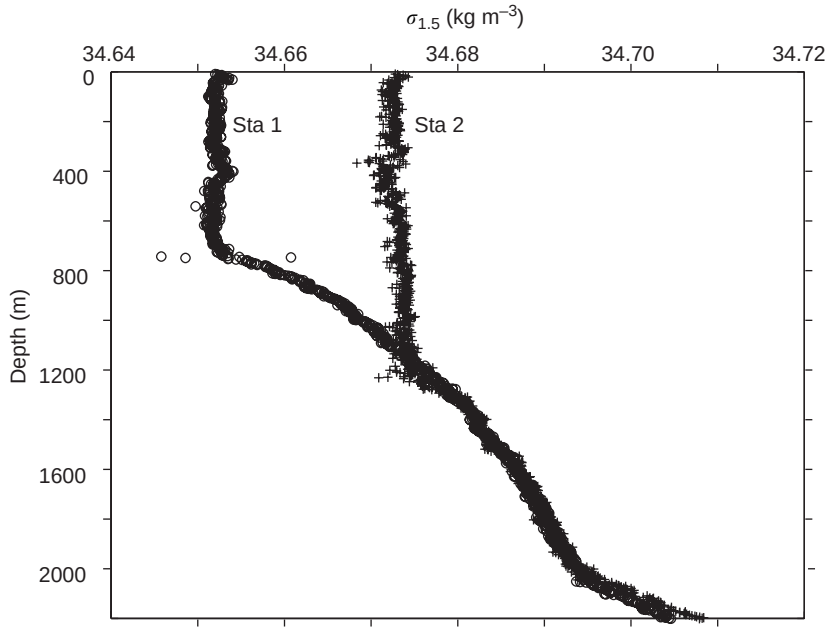

Figure 1 Vertical distribution of $\sigma_{1.5}$ obtained from R/V *Knorr* at 56.8°N, 54.2°W in the Labrador Sea on February 25 (Station 1) and March 8, 1997 (Station 2).

features provides the persistent heat loss from the same body of water that is needed to force convection to reach great depths.

The example of a deepening convection layer in **Figure 1** shows profiles of $\sigma_{1.5}$ ($\sigma_{1.5} + 1000 =$ potential density in kg m^{-3} referenced to 1500 decibars; 1 decibar corresponds to about 1 m) versus depth, on February 25 and March 8, 1997, in the Labrador Sea. The convecting layer is the approximately homogeneous layer next to the surface about 750 m deep with a $\sigma_{1.5}$ of 34.65 kg m^{-3} on February 25 (Station 1) and 1150 m deep and 34.67 kg m^{-3} 11 days later (Station 2). The buoyancy that was removed between the two profiles is proportional to the area between them, i.e.

$$\text{buoyancy} = (g/\rho_0)\int \Delta\rho \, dz$$

where g (10 m s^{-2}) is the acceleration due to gravity, ρ_0 (≈ 1034 kg m^{-3}) is the reference density, z is the depth and $\Delta\rho$ is the difference in density between Stations 1 and 2. For the two stations illustrated this calculation yields a buoyancy loss of 0.17 m^2 s^{-2}. By ignoring the small effect of evaporation, precipitation, and any advection, this buoyancy loss can be assumed to be due solely to heat loss from the surface. The loss is converted to joules by dividing by $g\alpha/\rho_0 c$ where g and ρ_0 are as before and α (about 10^{-4} °C^{-1}) is the thermal expansion of water and c (4.2 kJ kg^{-1} °C^{-1}) is the specific heat of sea water at constant pressure. The conversion suggests that a heat loss of about 0.68×10^9 J m^{-2} was required to remove the buoyancy between the two dates. Over the 11 days between the observations this heat loss is equivalent to an average rate of heat loss of 715 W m^{-2}. By a similar calculation, the heat loss required to increase the depth of convection to 2000 m would have been about 1.2×10^9 J m^{-2} or 460 W m^{-2} over a month.

If the profiles in **Figure 1** had been obtained during an era of mild winters rather than during one of abnormally severe winters they probably would have exhibited a markedly lower density in the upper layers. This might occur because of abnormally large freshwater flows into the surface layers due to increased outflows from the Arctic, warmer summers or a multiyear period of restratification following a vigorous period of convection. As the lower density represents 'extra' buoyancy to be removed before convection can proceed to greater depths, the ultimate depth of the convecting layer will be less in this situation, for a given heat loss, than in the illustrated one. Thus the ultimate depth of the convecting layer during a winter depends on the total amount of buoyancy lost from the sea surface and the distribution of that buoyancy with depth.

The distribution of the newly convected water in two dimensions is illustrated in the contour plot of salinity across the Labrador Sea in **Figure 2**. These data were obtained in July following the exceptionally cold winter of 1992–93. The water

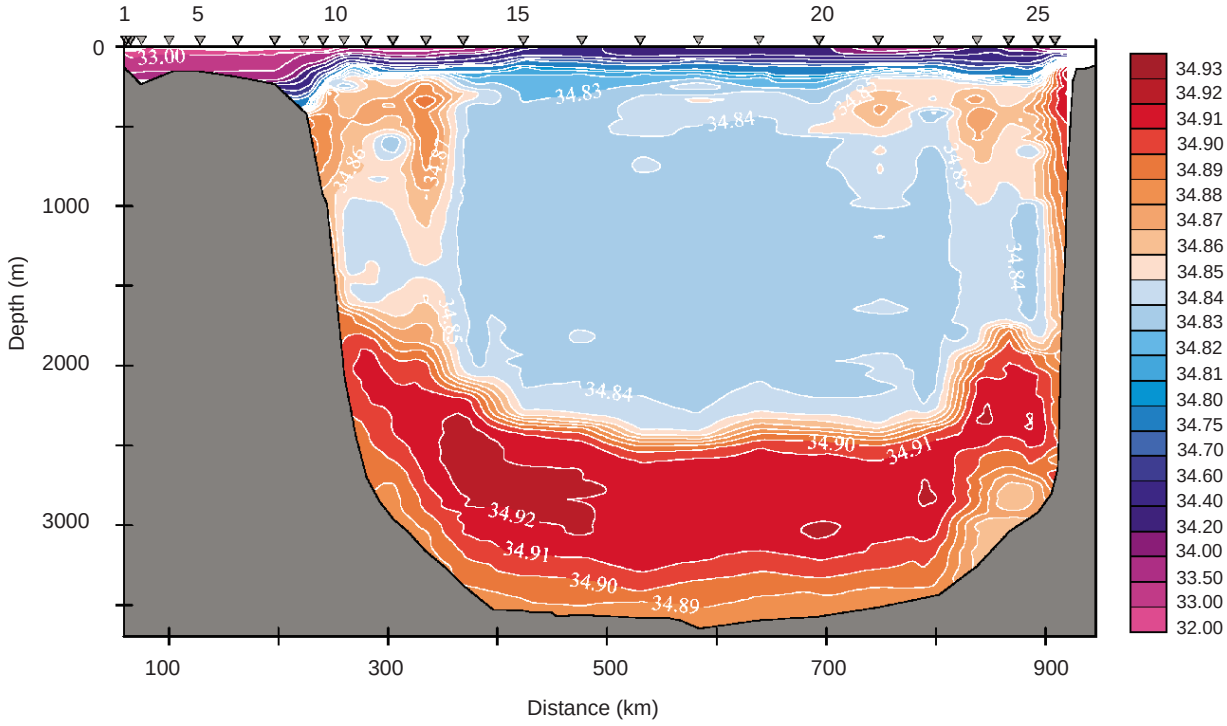

Figure 2 Salinity distribution across the Labrador Sea between 53.0°N, 55.5°W and 60.6°N, 49.3°W obtained between June 19 and 23, 1993. The water between 500 m and 2200 m in the central part of the section is unusually homogeneous because of deep convective mixing during the severe winter of 1992–93. The CTD station positions are indicated by numbered triangles along the surface.

mass resulting from convection is the large volume of nearly homogeneous water lying between 360 and 800 km on the horizontal scale and between 500 and 2300 m in the vertical. Because of its large volume, unique properties, and the fact that it spreads beyond its region of formation, this water is known as Labrador Sea Water. The upper layer (0–500 m) in the central part of the section is clearly not as well mixed as the layer between 500 and 2300 m. This is because the observations were obtained in July about 3 months after deep convection ceased at the end of the cooling season, about April 1. Since that time the surface layer has been flooded with fresh water derived from melting ice and river runoff. Also, the layer below this low salinity surface layer, to about 500 m, has been invaded by higher salinity water from the right (north-east) and to a lesser extent the left (south-west).

The newly formed Labrador Sea Water is a mixture of all the water down to 2300 m including the water in contact with the atmosphere at the surface. In these uppermost layers the concentration of gases such as oxygen, carbon dioxide, tritium, and chlorofluorocarbons (CFCs) are at or near equilibrium with the atmosphere. By transporting these gases down from the upper layers of the ocean to intermediate depths, convection provides a mechanism to ventilate the deeper layers, which is one of the most important consequences of deep convection. Dissolved oxygen, for example, is slowly used up in the deep ocean by biological processes and would eventually vanish without the renewal via convection. Also most of the carbon dioxide ever put in the atmosphere by volcanoes since the formation of the Earth became dissolved in the ocean and is now contained in sediments in the bottom of the ocean. As combustion of fossil fuels over the earth raises the carbon dioxide content of the atmosphere it is important to understand the rate at which this gas is entering the deeper layers of the ocean through processes such as deep convection (*see* **Carbon Cycle**).

Subsequent to formation, Labrador Sea Water spreads to other regions of the ocean at intermediate depths. Knowledge of the speed of this flow and its influence increased during the 1990s due to the widespread high quality observations of temperature, salinity, and CFCs across the North Atlantic obtained under the international World Ocean Circulation Experiment. The newly ventilated water formed in the Labrador Sea during the severe winters of the early 1990s moved across the North Atlantic at about 2 cm s^{-1}. This speed is about three to four times greater than the previous estimate,

leading to the conclusion that the intermediate flows are much faster than previously thought. A comparison of six decades of data from the Labrador Sea and from the subtropical waters near Bermuda suggest that the products of deep convection in the Labrador Sea impact the waters off Bermuda after about 6 years.

Plumes – the Mixing Agent

Convection begins to increase the depth of the mixed layer in the Labrador Sea near the end of September when the surface net buoyancy flux from the surface turns from positive to negative. Deepening continues until about the end of March when the buoyancy flux again becomes positive. When convection is active, water at the surface becomes denser than the underlying water and descends in plumes. This water is replaced by slightly lighter water rising toward the surface. The physical features of the convecting water including the plumes and the water between have been the subject of a number of investigations; most notably by the group of scientists at Kiel working in the Golfe du Lion in the Mediterranean Sea with moored acoustic Doppler current profilers (ADCP) and current meters. The cartoon in **Figure 3** summarizes some of the main features of plumes and the mixing layer.

At the surface is the thermal boundary layer where the water is losing heat/buoyancy to the atmosphere. Water in this layer is, on average, slightly denser than in the mixed layer beneath and descends into the mixing layer within plumes which have a horizontal dimension of about 1 km, approximately equal to that vertical extent, i.e. an aspect ratio of ≈ 1. The average rate of descent within the

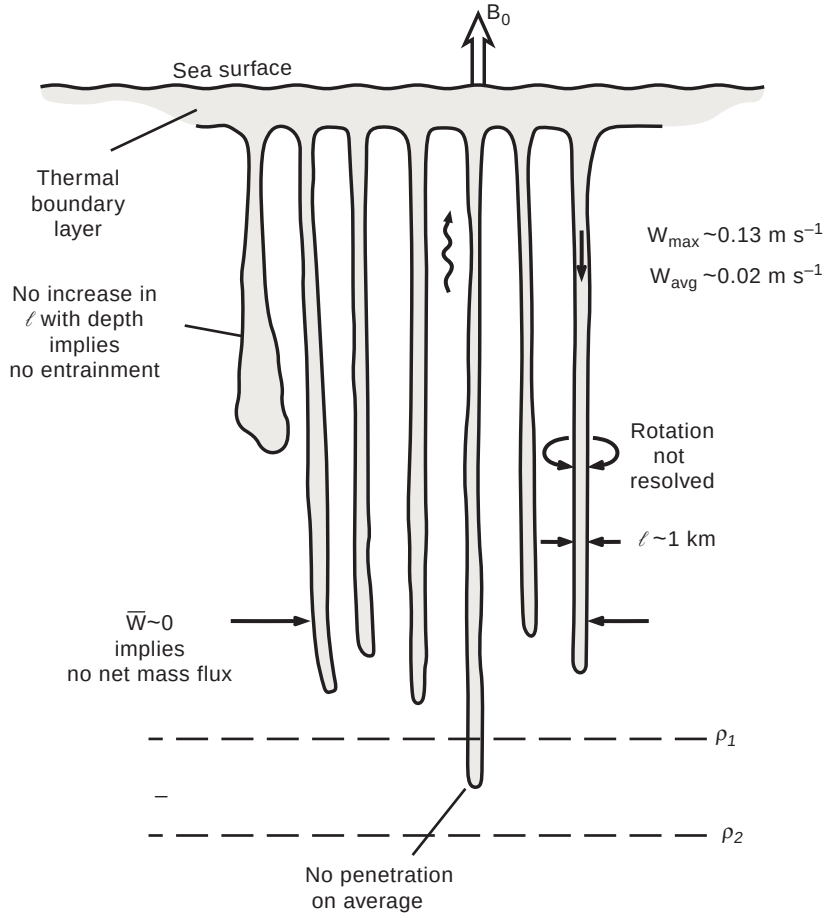

Figure 3 A schematic diagram of a ≈ 1000 m convecting layer indicating approximate values for features of individual plumes including the horizontal scale, vertical downward velocity, rotation, and entrainment. Across the patch of convecting water there is no net vertical mass flux and no significant penetration into the layers of denser water beneath the convecting layer. Buoyancy (B_0) lost from the surface creates the thermal boundary layer in the upper ≈ 100 m where the denser water is formed which sinks within the plumes. The wiggly up arrow indicates the (slow) upward flow that replaces the (relatively fast) downward flow within the plumes. Note that the horizontal scale in the figure is ≈ 50 times the vertical scale.

plumes is about $0.02\,m\,s^{-1}$ while the maximum is $\approx 0.13\,m\,s^{-1}$. Rotation of the plumes, due to the horizontal component of the Coriolis force, is expected because water must converge into the plume at its top and presumably diverge out of it near the bottom. However, this effect has not yet been conclusively observed in the field although it has been observed in laboratory experiments and in numerical simulations. Another effect that has not been observed is an increasing horizontal dimension with depth which is expected if water is entrained into the plumes as they descend, or if they decelerate as they go deeper.

Observations also indicate that there is no net vertical mass flux within a convecting region or patch. This appears to have solved the long-standing puzzle of whether the descending water was replaced by rising water between the plumes or by converging flow in the upper layer and diverging flow in the deep layer. Finally, on average, the plumes are not penetrative, i.e. the plumes do not have enough energy to descend into water that is denser than the water within the plume. One consequence of this is illustrated in **Figure 1** by the fact that the bottom of the mixing layer at Station 2 lies on the $\sigma_{1.5}$ versus depth curve observed earlier on February 25. If convection was penetrative the bottom of the mixed layer on March 8 would lie below this curve and the $\sigma_{1.5}$ versus depth gradient at the bottom of the mixing layer would be greater than when it was observed earlier. The plumes in the cartoon suggest that there should be a high correlation between fluctuations in temperature and vertical velocity. However, recent measurements from drifting floats indicate this correlation to be weak, thus making the cartoon a rather simplified view of the true situation. In reality the plumes are probably not vertical over the full depth of the convecting layer but contorted by the larger-scale flows.

A direct view of the motion within convecting plumes has recently been obtained from freely drifting floats. When one of these is launched it immediately sinks to a predetermined depth below the convecting layer where it remains for typically 7 days while its buoyancy adjusts. At the end of this period its buoyancy is decreased slightly and the float rises into the convecting layer. A large attached drogue then causes the float to be moved up and down with the vertical motions of convection. In the Labrador Sea over 25 days in February and March 1997 the maximum vertical velocity observed by a set of these floats was downward at $0.2\,m\,s^{-1}$ with a rms value for all the observations of $0.02\,m\,s^{-1}$. This is equivalent to a round trip of the convecting layer of 1 day for the average water parcel. On a number of occasions the floats were seen to penetrate below the average bottom of the mixing layer. Contrary to the conclusions mentioned above that the convection is not penetrative, this suggests that a certain amount of plume penetration into denser layers does occur.

Temperature and Salinity Variability

Year-long time-series records of temperature and salinity obtained in the middle of the Labrador Sea indicate that there is a marked increase in temperature and salinity variability during and following convection. This is evident in the temperature record in **Figure 4** obtained at 510 m in 1994–95. Between June and the middle of February the temperature sensor is below the mixed layer and the temperature slowly increases by about 0.2°C. In mid-February the temperature drops by about 0.4°C as the deepening convecting layer reaches the depth of the sensor. At this time the magnitude of the variations in temperature suddenly increase and continue at a high level for a number of weeks. Spectra calculated from 85-day pieces of this record before and after the arrival of the convection layer show a broadband fourfold increase in the spectral energy of the variability after the sensor is immersed in the mixed layer. Time-series of the energy show a peak in February shortly after the mixed layer arrives followed by a decline to 1/30th of the peak value by the end of the record in June.

Similar fluctuations occur in salinity and are largely in phase with those in temperature. **Figure 5** shows temperature versus salinity plots at four depths during 21 days in March 1995 when convection was proceeding to about $\approx 2000\,m$. During this time period density at each of these levels was relatively constant in time. In the figure the hourly observations at each depth show the extent of the fluctuations in temperature and salinity and the fact that they are largely parallel to the constant density surfaces; the T–S fluctuations tend to be parallel to the isopycnals. The most probable explanation for the fluctuations is that they are horizontal variations in temperature and salinity being swept past the mooring by the current. One suggestion is that these variations reflect horizontal variability in the depth of convection. However, recent work in the mixed layer of the tropical Pacific demonstrates that compensating horizontal variations in temperature and salinity may be ubiquitous features of the mixed layer whether it is convecting or not. These results lead to the alternative suggestion that the compensating temperature and salinity

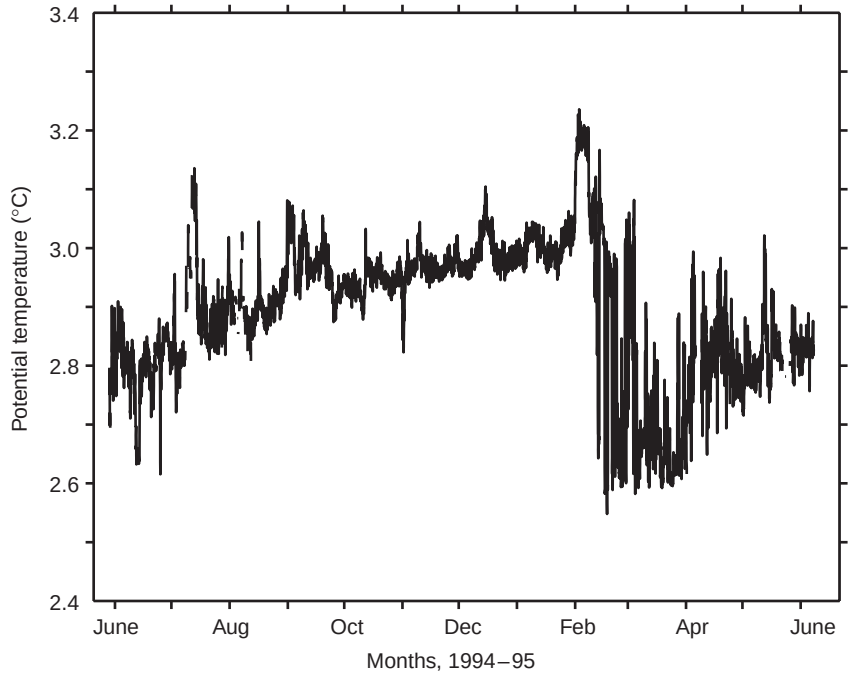

Figure 4 A 1 year record of temperature at 510 m in the central Labrador Sea illustrating the increase in variance during and after the mixed layer reaches the depth of the instrument in early February 1995 plus the sudden upward shift in temperature near April 1 associated with the end of convection.

variations exist in the wind-mixed surface layer before deep convection begins and are propagated downward by the convection.

When convection stops, the vertical density stratification is reestablished in the surface layers and the horizontal variations that appeared during convection are no longer renewed. Those variations existing when convection ends are then slowly mixed away by turbulent eddies leading to the decay in the amplitude of the fluctuations as observed in the time-series. Assuming a horizontal scale L of 100 km for the region of convection with its small-scale horizontal variations, the timescale of eddy mixing will be about L^2/K_H where K_H, the horizontal eddy diffusivity, is about $10^3\,\mathrm{m^2\,s^{-1}}$. This gives a timescale for the horizontal mixing of about 4 months, which is about the decay time observed in the records.

Restratification

At the end of the cooling season, vertical mixing due to convection ceases and its dominant influence on mid-depth water properties ends. This also marks the beginning of the restratification process during which the vertical stratification existing prior to the homogenization begins to be reestablished. Two timescales seem to be involved. At the end of convection a rapid restratification occurs which is indicated by sudden shifts of variables such as temperature. One example is indicated in **Figure 4** by the increase of 0.2°C near April 1 following roughly 6 weeks of convective activity at this depth. It is not clear if this increase indicates an end to convection over a large area, or the advection of a stratified nonconvecting water column to the observation site. The first option, however, seems more likely as the end of convection appears in other records as a rapid increase in stratification especially in the upper layers. For example, a tomographic array in the Golfe du Lion observed a roughly 40 day restratification period following convection. This seems to be the only observation of restratification over a large area. Another example is the record from a PALACE (profiling autonomous Lagrangian circulation explorer) in the Labrador Sea which shows, during 2 consecutive years, a sudden transition between the low stratification associated with convection and a stratified water column. This record is admittedly like a mooring, from a single point, but it does give a consistent picture in the 2 years.

A recent numerical model of the restratification process may describe this rapid phase. It has a homogeneous cylinder of water floating in an ocean of constant stratification. The density gradient between the cylinder and the surrounding ocean gives rise to a narrow cyclonic current which breaks up via

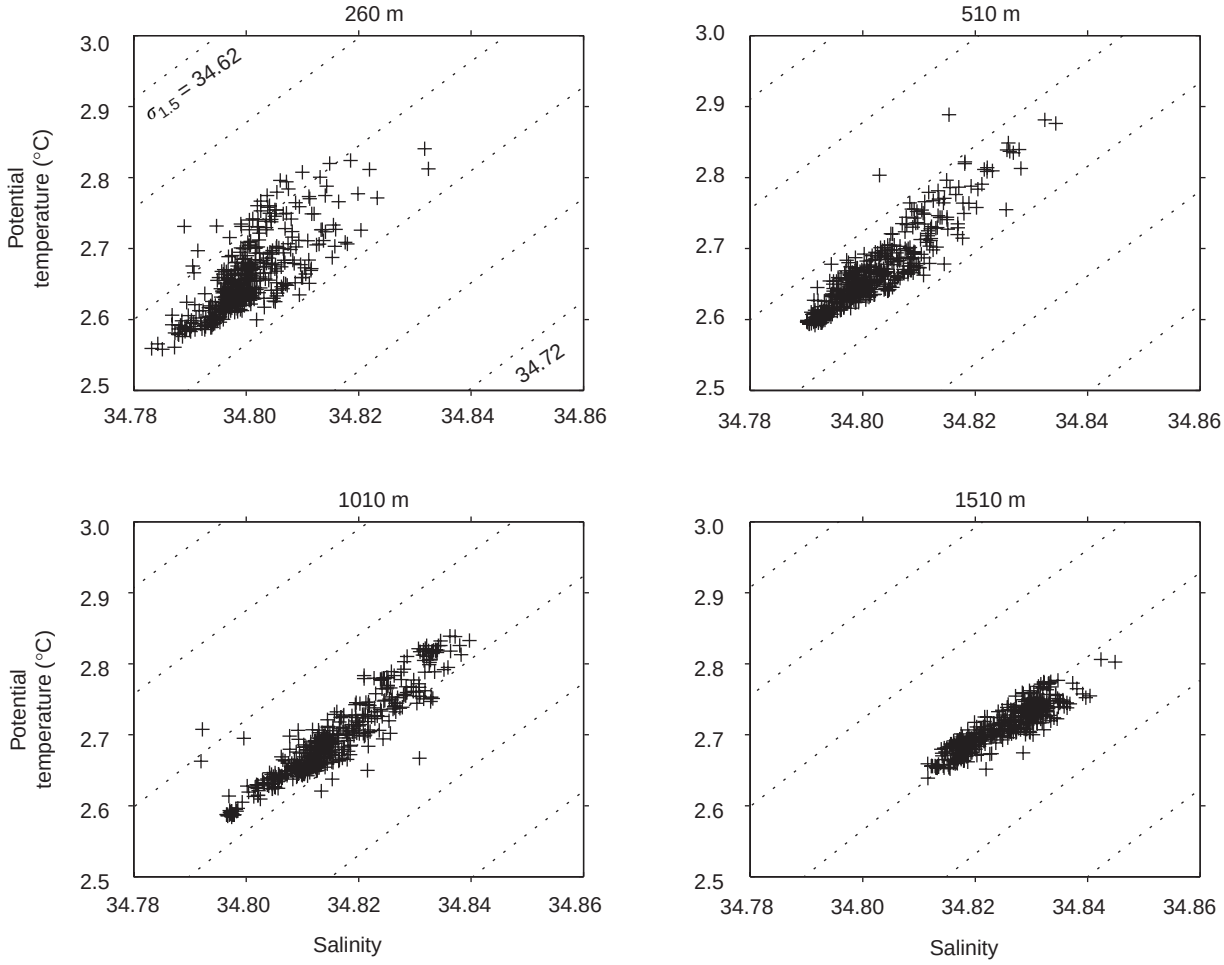

Figure 5 Temperature versus salinity diagrams based on data obtained at 260, 510, 1010, and 1510 m in the central Labrador Sea , between March 12 and April 2, 1995, during the final stage of convection when the density at these depths remained relatively constant.

baroclinic instability into baroclinic eddies. These mix the homogeneous water horizontally with the stratified waters and so dissipate the homogeneous cylinder in timescale τ. For the special case where the stratification in the water surrounding the homogeneous cylinder is concentrated in the upper layer h:

$$\tau \approx 56\,\mathrm{r}/(\mathrm{h}\Delta\mathrm{b})^{1/2}$$

where r is the radius of the homogeneous cylinder, h is the depth of the upper stratified water bounding the homogeneous cylinder and Δb is the difference in density between the homogeneous water and the surrounding water in buoyancy units (i.e. $\Delta\mathrm{b} = \mathrm{g}\Delta\rho/\rho_0$). For the Labrador Sea where $\mathrm{h} \approx 500\,\mathrm{m}$, $\Delta\mathrm{b} \approx 2 \times 10^{-3}\,\mathrm{m\,s^{-2}}$ and $\mathrm{r} \approx 100\,\mathrm{km}$; $\tau \approx 65$ days. This result, being of the same order as the observed rapid changes in stratification, suggests that the model may be appropriate to explain the observations.

The long timescale of restratification has now been observed in the Labrador Sea. Observations have been made continuously over one summer and intermittently over a few successive years. Changes over the summer of 1996 are illustrated in **Figure 6** by the depths of four of the isopycnals within the upper 1000 m. At stations between 400 and 600 km the isopycnal depths increase significantly between May and October while the 27.72 and 27.74 $\mathrm{kg\,m^{-3}}$, surfaces between 650 and 790 km, show a decrease in depth. These changes suggest that lighter water, from beyond the region of deepest convection (400–600 km), moves into the upper water column in the region of deepest convection while denser water in the region of deepest convection moves outward toward the boundaries at mid-depth.

Restratification over a number of years is illustrated in the time series of $\sigma_{1.5}$ through the 1990s in **Figure 7**. In the early years of the decade the water

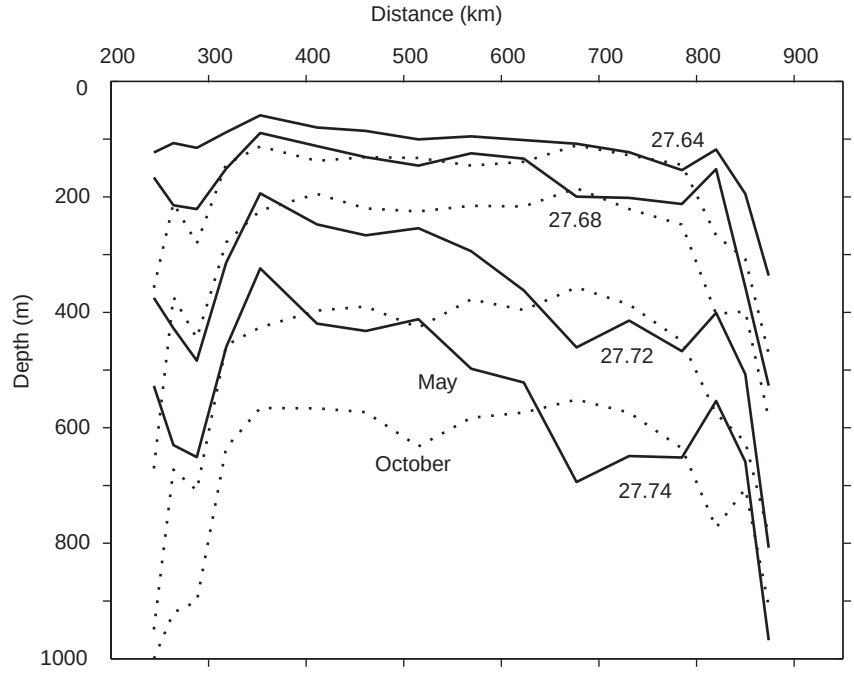

Figure 6 Four surfaces of constant σ_0 (potential density anomaly relative to 0 m) across the Labrador Sea based on CTD data collected in May 1996 (solid lines) and October 1996 (dotted lines).

produced by the convection, indicated by the layer of low vertical gradient, lies within the 34.64 and 34.70 kg m^{-3} surfaces. Between 1990 and 1994 the volume of this water remains roughly constant but the value of $\sigma_{1.5}$ at the core increases from 34.67 to 34.69 kg m^{-3} as the winters became more severe and the convecting layer continued to deepen into the stratified layer below. In the years following 1995, convection was limited to 1000–1500 m. The deep reservoir of 'homogeneous' water was thereby

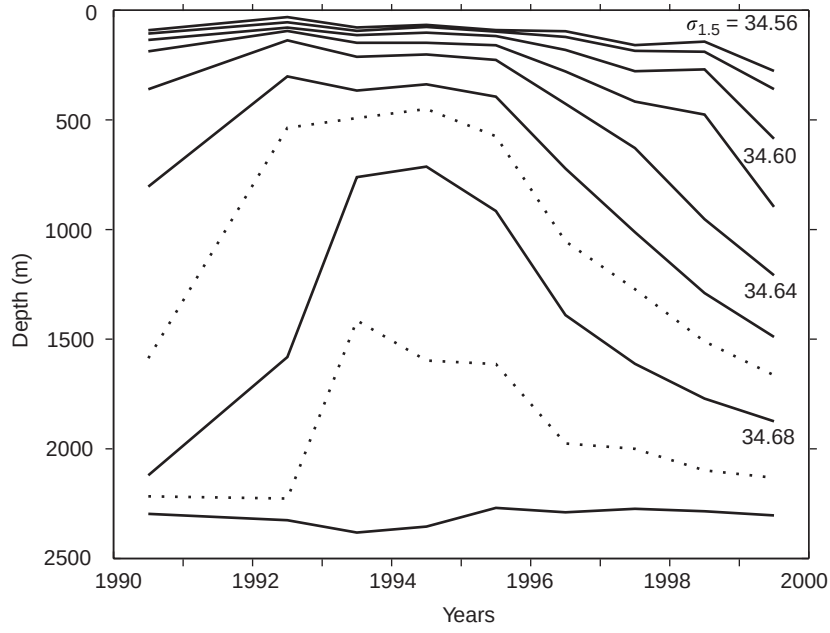

Figure 7 Depths of $\sigma_{1.5}$ surfaces in the middle of the Labrador Sea through the 1990s based on CTD data collected in May or June of each year.

isolated below the convecting layer and slowly decreased in volume with each passing year as it drained away. This decrease in volume was balanced by an increase in the volume of lighter more stratified water in the upper layers from the boundaries. The large interannual variation in the volume of the Labrador Sea Water illustrated in this figure is a well known property of the water mass; however, its effects on the large-scale ocean currents and processes are not yet well understood.

Discussion

While the focus of this article has been on the Labrador Sea, numerous aspects of the convective processes discussed here also apply to the other two locations of open-ocean convection in the North Atlantic: the Greenland Sea and the Mediterranean Sea. But as there are common threads to the overturning in these seas there are also significant regional differences. The Greenland Sea is unique in that ice plays a significant role in the preconditioning phase. The deepest convective overturning occurs in late winter just after the ice-free 'Nord Bukta' region opens up. In the Mediterranean the winds are more localized than in the other two regions. This clearly influences the convection, as the region of deepest mixed layers generally lies in the path of the Mistral winds. Furthermore, these winds are rarely cold enough to cause convection during daylight hours, so the Mediterranean has a daily cycle of overturning that is not present in the other two seas. Also, the impact of the basin-scale North Atlantic Oscillation wind pattern influences the Labrador and Greenland Seas to a much greater extent than the Mediterranean. Finally, the dimensions of the convection zones and convected water masses differ greatly. In the Mediterranean, the convecting patch is of order 50 km wide; in the Greenland Sea it is of order 100 km wide, and in the Labrador Sea the zone of convection approaches 500 km in width, and includes the boundary currents.

Convection at each of these three Atlantic sites contributes to the global meridional overturning circulation, although the quantitative measures are not yet known. In the Greenland Sea particularly, the deep convection into the cyclonic gyre seems rather isolated from the processes that produce the dense overflows. Mediterranean Water and Labrador Sea Water both make an obvious contribution to the Upper North Atlantic Deep Water, respectively, as high and low salinity endpoints. Distant identification of Labrador Sea Water is through its low salinity; potential vorticity; low nutrient concentration; high dissolved oxygen, tritium, and CFCs. Along the western boundary velocity and CFC maxima associated with Labrador Sea Water have been observed near Abaco, nearly 5000 km south. For the era ending in 1977 a dilution of the tritium maxima of the deep western boundary currents by factors of order 10 was observed, from the subpolar gyre to the Blake-Bahama Outer Ridge. This suggested dilution and delay (by recirculation) mechanisms *en route*.

Model studies suggest that when convection is initiated or increased at the high-latitude source, a pressure wave propagates south along the western boundary, as a topographic Rossby wave, well before the arrival of tracer-tainted, identifiable water mass. Such model studies point out that sloping topography acts as a wave guide, and rather gently leads dense water masses equatorward from high latitude, as they slowly sink. Thus, 'sinking' is minimal in the near-field of the convection, but occurs downstream. Production of kinetic energy of the overturning circulation by potential energy created by buoyancy forcing requires that dense water sink and less dense water rise, but the sites of sinking and rising are, at least in model studies, often distant from the convection. In a diapycnal/epipycnal coordinate system, however, convection is more locally associated with time-averaged diapycnal transport ('water-mass conversion'). Such analyses are beginning to be carried out with models and are an insightful way to approach the link between convection, sinking, and global meridional overturning.

Thus we are still seeking to quantify production rates of the constituent water masses of the global meridional overturning. Outward transport of Labrador Sea Water is even difficult to define, because of extensive recirculation within the subpolar gyre, and entrainment once the water mass has left the subpolar gyre. Estimates have ranged from < 1 Sv to > 10 Sv. Much also remains unknown about the detailed geography of deep convection and circulation. In the Labrador Sea, both interior and boundary currents are known to participate in the deep convection (estimates of 1–2 Sv of boundary current production). However, the boundary current, is shielded from deep convection by low salinity shelf waters at some sites. Where the circulation crosses from Greenland to Labrador, the boundary currents broaden and slow down, and are generally exposed to some of the most intense air–sea heat flux in the sea; there and over the wide continental slope near Labrador, convection may be particularly deep.

Direct velocity and transport measurements are needed to augment water mass observations. Unfortunately the Lagrangian movement of water masses

is difficult to observe even with modern 'quasi-Lagrangian' floats and drifters. A recent description of the Labrador/Irminger Sea circulation from PALACE floats notes that 'no floats travelled southward to the subtropical gyre in the deep western boundary current, the putative main pathway of dense water in the meridional overturning circulation'. If the boundary current is concentrated to a narrow width, for example at the Flemish Cap, then these profiling floats may have difficulty staying within it; tracer observations assure us that the transport does in fact take place.

See also

Carbon Cycle. Current Systems in the Mediterranean Sea. Mediterranean Sea Circulation. Rossby Waves. Sub-sea Permafrost. Thermohaline Circulation.

Further Reading

Lazier JR, Pickart RS, Rhines PB (2001) Deep convection. In: *Ocean Circulation and Climate – Observing and Modelling the Global Ocean*. London: Academic Press.

Lilly J, Rhines P, Visbeck M *et al.* (1999) Observing deep convection in the Labrador Sea during winter 1994–1995. *Journal of Physical Oceanography* 29: 2065–2098.

Marshall J and Schott F. (1999) Open-ocean convection: observations, theory and models. *Reviews of Geophysics* 37: 1–64.

Schott R, Visbeck M and Send U (1994) Open ocean deep convection, Mediterranean and Greenland Seas. In: Malanotte-Rizzoli P and Robinson AR (eds) *Ocean Processes on Climate Dynamics: Global and Mediterranean Examples*, pp. 203–225. Dordrecht: Kluwer Academic Publishers.

Lab Sea Group (1998) The Labrador Sea Deep Convection Experiment. *Bulletin of the American Meteorological Society* 79: 2033–2058.

DEEP SUBMERGENCE, SCIENCE OF

D. J. Fornari, Woods Hole Oceanographic Institution, Woods Hole, USA

doi:10.1006/rwos.2001.0424

Introduction

The past half-century of oceanographic research has demonstrated that the oceans and seafloor hold the keys to understanding many of the processes responsible for shaping our planet. The Earth's ocean floor contains the most accurate (and complete) record of geologic and tectonic history for the past 200 million years that is available for a planet in our solar system. For the past 30 years, the exploration and study of seafloor terrain throughout the world's oceans using ship-based survey systems and deep submergence platforms has resulted in unraveling plate boundary processes within the paradigm of sea floor spreading; this research has revolutionized the Earth and Oceanographic sciences. This new view of how the Earth works has provided a quantitative context for mineral exploration, land utilization, and earthquake hazard assessment, and provided conceptual models which planetary scientists have used to understand the structure and morphology of other planets in our solar system.

Much of this new knowledge stems from studying the seafloor – its morphology, geophysical structure, and characteristics, and the chemical composition of rocks collected from the ocean floor. Similarly, the discoveries in the late 1970s of deep sea 'black smoker' hydrothermal vents at the midocean ridge (MOR) crest (**Figure 1**) and the chemosynthetic-based animal communities that inhabit the vents have changed the biological sciences, provided a quantitative context for understanding global ocean chemical balances, and suggest modern analogs for the origin of life on Earth and extraterrestrial life processes. Intimately tied to these research themes is the study of the physical oceanography of the global ocean water masses and their chemistry and dynamics, which has resulted in unprecedented perspectives on the processes which drive climate and climate change on our planet. These are but a few of the many examples of how deep submergence research has revolutionized our understanding of our Earth and ocean history, and provide a glimpse at the diversity of scientific frontiers that await exploration in the years to come.

Enabling Deep Submergence Technologies

The events that enabled these breakthroughs was the intensive exploration that typified oceanographic expeditions in the 1950s to 1970s, and focused development of oceanographic technology and instrumentation that facilitated discoveries on many